NOAA Technical Memorandum ERL PMEL-85

AN ATTEMPT TO EVALUATE THE EFFECTS OF AN ANTI-TURBIDITY SYSTEM ON SEDIMENT DISPERSION FROM A HOPPER DREDGE

Kisaburo Nakata
Katsuya Tsurusaki
National Research Institute for Pollution and Resources
Ministry of International Trade and Industry, Japan

Yoshikuni Okayama
Port and Harbor Research Institute
Ministry of Transport, Japan

J. William Lavelle
Pacific Marine Environmental Laboratory

Pacific Marine Environmental Laboratory
Seattle, Washington
January 1989

UNITED STATES
DEPARTMENT OF COMMERCE

C.William Verity
Secretary

NATIONAL OCEANIC AND
ATMOSPHERIC ADMINISTRATION

William E. Evans
Under Secretary for Oceans
and Atmosphere/Administrator

Environmental Research
Laboratories

Vernon E. Derr,
Director

NOTICE

Mention of a commercial company or product does not constitute an endorsement by NOAA. Use of information from this publication concerning proprietary products or the tests of such products for publicity or advertising purposes is not authorized.

Contribution No. 1060 from NOAA/Pacific Marine Environmental Laboratory

For sale by the National Technical Information Service, 5285 Port Royal Road
Springfield, VA 22161

CONTENTS

An Attempt to Evaluate the Effects of an Anti-Turbidity System on Sediment Dispersion from a Hopper Dredge

Kisaburo Nakata[1], Katsuya Tsurusaki[1], Yoshikuni Okayama[2], and J. William Lavelle[3]

ABSTRACT. Measurements were made during six hopper dredge operations to investigate the differences in plumes of overspilled particulates when the dredger was and was not using an anti-turbidity system. Observations for discharge rates of suspended solids were taken aboard the dredge ship while concentration samples of suspended solids were taken by survey boats in the plume and currents were metered by instruments on moorings. Measurements were given a common framework by the use of a dispersion model for the plume. Modeled and observational profiles match well when the rate of discharge is reserved as a fitting parameter. However, differences in results of the use and non-use of the anti-turbidity system are not discernible with the field data. Consequently, the model was used under identical advection and diffusion conditions to study the differences theoretically. Those numerical experiments suggest that there is an increase of about 25% in the amount of deposition in the immediate area of dredging with the anti-turbidity system, though the fractional amount of redeposition in both cases is small. The differences in results for the two systems calculated with the model depend on the assigned initial vertical distributions. Because these are poorly known at present, better definition of the differences with and without the anti-turbidity system await better measurements of the vertical distributions of suspended solids in the ocean immediately following discharge.

1. INTRODUCTION

Understanding the behavior of suspended solids in an estuary or a coastal region is important for evaluating their effects on the aquatic ecosystem. Suspended solids in the ocean reduce light penetration affecting the growth of phytoplankton, adsorb and concentrate some pollutants such as toxic chemicals, promote the consumption of great quantities of dissolved oxygen for oxidizing organic matter, and may have other effects yet to be identified. The overspill and dredgehead disturbance of the seafloor during dredging operations represent two localized sources of suspended solids to the marine environment. Thus, understanding the extent of the suspended-solids dispersion after dredging and results of possible mitigating procedures is highly desirable.

Any technique that reduces the dispersion of turbid water following a dredging operation is assumed to reduce the effects of dredging on the marine ecosystem. One of the new techniques to do so is an anti-turbidity system (hereafter, ATS), a system that reduces the amount of air entrained in hopper dredge effluent (Ofuji *et al.*, 1977; Okayama and Saotome, 1980). Air bubbles in hopper-dredge effluent promote the mixing of discharge upward from the discharge

[1] National Research Institute for Pollution and Resources, Ministry of International Trade and Industry, Japan
[2] Port and Harbor Research Institute, Ministry of Transport, Japan
[3] Pacific Marine Environmental Laboratory, National Oceanic and Atmospheric Administration, U.S.A.

depth to the surface. Reducing the amount of entrained air in the effluent with ATS should reduce overflow particulate concentrations near the surface and consequently the extent of their dispersion.

The effectiveness of the ATS concept can only be judged after field tests have been conducted. With this in mind, an experiment was designed to measure and compare suspended solids plumes resulting from dredging operations with and without the use of ATS. Results of that field experiment are summarized here. But the number of observations of the dispersion process with and without ATS were limited. The analysis of the data showed that the observations alone could not be used to identify definitely a reduction in the dispersion of the overflow particulates when ATS was employed. Using information coming from the tests, numerical experiments were subsequently conducted to examine theoretically the differences in particulate dispersion. These results are presented here too. The field work was conducted as a bilateral project of the Marine Mining Panel of the United States-Japan Cooperative Program in Natural Resources.

2. OBSERVATIONS

In order to evaluate the effectiveness of ATS, measurements were made during dredging operations in the vicinity of the Kanmon Channel over the period July 23-25, 1984. The experimental program consisted of observations taken under conditions of no overflow, overflow with the anti-turbidity system (ATS), and overflow without ATS (Table 1). The measurements included rates and particulate concentrations of discharge on the dredge ship and suspended

TABLE 1. Schedule of observations.

Experiment	Observing Period Day	Observing Period Time	Dredging Condition*
1	23 July 1984	10:15 ~ 12:45	I
2	23 July 1984	13:45 ~ 15:58	I
3	24 July 1984	10:30 ~ 12:28	II
4	24 July 1984	14:15 ~ 16:16	III
5	25 July 1984	10:10 ~ 12:20	III
6	25 July 1984	13:50 ~ 15:57	II

* I: No overflow from dredger
II: Overflow from dredger with ATS
III: Overflow from dredger without ATS

particulate concentration and current meter measurements over time in and around the effluent plume. Samples were also analyzed for particle sizes. The plume of solids actually originates both at the seafloor from the disturbance caused by the dredgehead and near the sea surface in the overflow of excess water. The primary interest in this work is the plume component contributed by overflow.

The measurements were made in coordination with operations of the hopper dredge KAIHO MARU. That ship was conducting maintenance dredging of the shipping lane entering Kanmon channel (Fig. 1). The dredge operating area was rectangular, having dimensions 1.3 km by 250 m with the long axis oriented in the direction 310°. Bottom sediments at this location are composed of silts and clays. The nominal depth in the dredge area is 15 m.

During each measurement period the KAIHO MARU made a "U"-shaped transit across the area, with each arm of the "U", about 1.3 km in length, oriented along the long axis of the dredge area and each arm separated by about 150 m. The normal dredging speed was 1.5 to 2.4 m/s. The hopper of the ship was large enough that along the first arm of each transit, no water was spilled overboard. Along the second arm, turbid water would overspill over a period of approximately 10 min and over a distance of about 1 km. A bottom disturbance would be created on each arm of the transit, but a surface plume would be created only on the second arm. On board the dredge ship time series of pumping rates and of suspended particulate levels at the dredgehead and at the overflow point were taken (Fig. 2 and Table 2).

TABLE 2. Measured concentrations of suspended solids around the dredgehead and in the overflow.

	Dredgehead		Overflow	
	Time	Concentration (ppm)	Time	Concentration (ppm)
Experiment 4, without ATS (Case A)	14:21	1,900		
	24	270		
	27	120		
	38	22,000	14:40	240,000
	42	10,000	42	3,900
	44	300	44	9,000
Experiment 6, with ATS (Case B)	14:00	6,500		
	03	3,100		
	06	4,000		
	16	15,000		
	18	7,000	14:18	120,000
	21	11,000	23	90,000
	24	3,900	26	78,000

During the transit of the KAIHO MARU along the second arm of the "U" through the dredge area, monitoring boats took up position in the wake of the dredger to sample the plume. Plume survey boats, six in number, established a picket line normal to the dredge track roughly at midlength along the line of discharge. Two drifting markers drogued at 2 or 5 m were deployed in the wake of the dredger to serve as position markers of the surface-plume centerline for the survey boats. The survey boats, attempting to maintain nearly fixed position one to another on a line normal to the drifting markers, pumped water samples over time from many depths. These samples were later analyzed for total suspended matter and for size distributions. In some of the experiments two survey boats broke from this pattern to tow transmissometers at several depths across the plume. From among the six sets of observations (Table 1), two data sets were selected to represent dispersion results with and without ATS and for use in conjunction with numerical experiments. These are Experiment 4, without ATS, hereafter called Case A, and Experiment 6, with ATS, hereafter called Case B. Further description of the field experimental program and a full report of all the measurements are available in the data report (Marine Mining Panel, 1984).

Measured concentrations of solids at the dredgehead and in the overflow water are given in Table 2. Concentrations at both points and in both tests varied greatly in time. Over a two-minute period concentrations varied from 3.9×10^4 to 2.4×10^5. Total flow rates of both starboard and port side pumps were also measured (Fig. 2). These pump rates were integrated over time to judge the time the hopper, having capacity of approximately 2×10^3, would overflow and to estimate the volume rate of the overflow thereafter. The capacity of the ship was such that the overflow occurred only on the second pass of the ship through the dredge area as previously mentioned.

The rate of solids discharge near the sea surface was estimated to be the product of the measured particulate concentrations and these spillage rates. The rate of suspended solids introduced into the water column at the dredgehead was estimated to be the product of the measured concentration at the dredgehead (Table 2) and the volume swept by the dredgehead per unit time. Table 3 gives estimates of the amounts discharged over fixed time intervals. These estimates suggest that nearly as much suspended solids are injected into the water column at the dredgehead as in the near surface overflow. For Case A, 87.5 mt are estimated to have been discharged in the overflow over a 9-min period, while in Case B 131.5 mt were discharged over a 10-min period.

Vertical distributions of suspended solids concentration at the plume center line measured over time are shown in Fig. 3 for Experiments 3-6 including Cases A and B. Ambient concentrations, also given in Fig. 3, are seen to range from 1.3 to 9.2 mg/l except very near the bottom. Once dredging occurs, the concentration of particulates in the water column is over ten-fold larger. Concentrations reach much lower levels over the 1.5-2 hours of observations. This reduction is in part caused by settling, but is also the result of horizontal dispersion for a source

TABLE 3. Estimated loadings of suspended solids at the seafloor and in the overflow during Cases A and B.

Experiment/ Source	Time (min)	Estimation Procedure	Load (mt)	Ship Speed (m/s)
CASE A:				
Dredgehead Outward	0~3	$180\ s \times 4\ m^2 \times 2.167\ m/s \times 1{,}900\ g/m^2$	2.9645	2.167
	3~6	$180\ s \times 4\ m^2 \times 2.167\ m/s \times 270\ g/m^2$	0.4213	2.167
	6~12	$360\ s \times 4\ m^2 \times 2.167\ m/s \times 120\ g/m^2$	0.3745	2.167
		subtotal	3.7603	
Dredgehead Return	16~20	$240\ s \times 4\ m^2 \times 1.970\ m/s \times 22{,}000\ g/m^2$	41.6064	1.970
	20~24	$240\ s \times 4\ m^2 \times 1.970\ m/s \times 10{,}000\ g/m^2$	18.9120	1.970
	24~29	$300\ s \times 4\ m^2 \times 1.970\ m/s \times 300\ g/m^2$	0.7092	1.970
		subtotal	61.2276	
Overflow	20~22	$(2{,}387\ m^2 - 2{,}052\ m^2) \times 240{,}000\ g/m^2$	80.4000	
	22~24	$(2{,}639\ m^2 - 2{,}387\ m^2) \times 3{,}900\ g/m^2$	0.9812	
	24~29	$(3{,}315\ m^2 - 2{,}639\ m^2) \times 9{,}000\ g/m^2$	6.0858	
		subtotal	87.4670	
Total			152.4549	
CASE B:				
Dredgehead Outward	0~5	$300\ s \times 4\ m^2 \times 2.407\ m/s \times 6{,}500\ g/m^2$	18.7746	2.407
	5~8	$180\ s \times 4\ m^2 \times 2.407\ m/s \times 3{,}100\ g/m^2$	5.3724	2.407
	8~12	$240\ s \times 4\ m^2 \times 2.407\ m/s \times 4{,}000\ g/m^2$	9.2429	2.407
		subtotal	33.3899	
Dredgehead Return	16~21	$300\ s \times 4\ m^2 \times 1.548\ m/s \times 15{,}000\ g/m^2$	27.8640	1.548
	21~23	$120\ s \times 4\ m^2 \times 1.548\ m/s \times 7{,}000\ g/m^2$	5.2013	1.548
	23~26	$180\ s \times 4\ m^2 \times 1.548\ m/s \times 11{,}000\ g/m^2$	12.2602	1.548
	26~30	$240\ s \times 4\ m^2 \times 1.548\ m/s \times 3{,}900\ g/m^2$	5.7957	1.548
		subtotal	51.1212	
Overflow	20~23	$(2{,}485\ m^2 - 2{,}052\ m^2) \times 120{,}000\ g/m^2$	51.9120	
	23~28	$(3{,}197\ m^2 - 2{,}485\ m^2) \times 90{,}000\ g/m^2$	64.1430	
	28~30	$(3{,}396\ m^2 - 3{,}197\ m^2) \times 78{,}000\ g/m^2$	15.4670	
		subtotal	131.5220	
Total			216.0331	

that is initially only a few tens of meters wide. Complete sections of suspended solids at each measurement time are to be found in the data report (Marine Mining Panel, 1984).

The discharge from the dredger occurs at a depth of 5.5 m below the sea surface. In all panels of Fig. 3, elevated concentrations of solids are found near the surface. It is believed that this is caused by vertical mixing induced by the screw-propeller of the dredge ship and, in the case of operations without ATS, by the entrained air bubbles in the effluent. On the other hand, the vertical concentration profiles (Table 4) suggest that there is slightly more particulate loading in the near-surface ocean without ATS than with it and that concentration profiles are more skewed toward the seafloor with ATS than without it. This result is consistent with the design intent for the ATS system. If air bubbles are part of the discharge, the overflow particulates have more tendency to rise toward the sea surface than they do when the bubbles have been removed by the anti-turbidity system.

In order to understand the changes in suspended solid profiles over time, it is necessary to differentiate changes due to settling from those that result from horizontal dispersion. To achieve this, some information about the settling velocity of the particles must be known. A direct measurement of settling velocity was not possible in the context of these experiments. In lieu of settling velocity, particle size measurements were made. Particle sizes were then used to estimate settling velocity in the manner described below.

Size data of suspended solids at the dredgehead, in the overflow water, and within the plume itself for Cases A and B is given as cumulative distributions in Fig. 4. Effective spherical diameters of the particles were determined by Coulter Counter. Substantial differences of the distributions between Cases A and B or sample locations is not recognizable in the data (Fig. 4). Diameters of particles in every case are less than 80 μm and more than 90% of the samples have diameters greater than 4 μm (Fig. 4). The median diameter of particles is about 10 μm.

TABLE 4. Measured vertical distributions of concentration and loading percentages for Cases A and B at the start of each survey.

	Case A		Case B	
Depth (m)	Concentration (ppm)	Weight (%)	Concentration (ppm)	Weight (%)
0 ~ 2	53.2	17.7	45.3	12.5
2 ~ 5	58.1	29.0	51.9	21.4
5 ~ 6	63.5	10.6	58.7	8.1
6 ~ 9	59.8	29.9	66.7	27.5
9 ~ 12	25.7	12.8	74.0	30.5

Currents in the area at the time of each experiment were measured with four meters located on a single mooring. Meter depths were 3 and 5 m below the surface and 1 and 3 m above the bottom. The water-column depth over the dredge area ranged from 13-16 m. The current meter data in all cases indicated a shear in both magnitude and direction over the water column (e.g. Fig. 5). For example, in Case A mean current speeds at the upper two meters were 34 and 21 cm/s, while for Case B both near-surface speeds were 28 cm/s (Fig. 6). At the near bottom meters mean current speeds were 5 and 6 cm/s for Case A and 7 and 9 cm/s for Case B (Fig. 6). Directional shear of more than 120 degrees between top and bottom meters was also common (Fig. 5). Such large directional shear makes difficult the field task of acquiring a full three-dimensional moving picture of a plume with point or profile measurements.

3. SUSPENDED SOLIDS DISPERSION MODEL

A model of particulate dispersion has been used to provide a framework for the interpretation of the measurements. The model is based on the statement of mass conservation for solids settling with a velocity w_s

$$\frac{\partial C}{\partial t} + \frac{\partial (uC)}{\partial x} + \frac{\partial (vC)}{\partial y} + w_s \frac{\partial C}{\partial z} = K_x \frac{\partial^2 C}{\partial x^2} + K_y \frac{\partial^2 C}{\partial y^2} + K_z \frac{\partial^2 C}{\partial z^2} + Q \qquad (1)$$

where x, y, and z are Cartesian coordinates, t is time, C is suspended solids concentration, u and v are advection velocities in the x and y direction respectively, w_s is the settling velocity of particulates, K_x, K_y and K_z are eddy diffusivities in the x, y, and z direction, and Q is the rate of loading of solids into the water column. The equation is solved with a no-flux condition at the sea surface, a zero gradient condition at the bottom, and a condition of no horizontal particulate flux into the calculational domain. This last condition is compatible with allowing only downstream advective transport of solids.

Equation 1 is written for a single settling component. For the case of a real discharge composed of particles of many sizes (e.g. Fig. 4), model results for individual settling velocities are summed after weighting the rate of loading by the mass fraction that particles of a single settling velocity represent in the total discharge. For the calculations here, the suspended solids are treated as if their distribution (Fig. 4) were composed of three sizes only--5, 10, and 30 μm. The fractional contribution of each size to the whole is based on the curves of Fig. 4. The settling velocity of each of the three size components is based on the Stokes equation (e.g. Batchelor, 1984). Assuming the density of solids to be 2.65 g/cm^3, the corresponding settling velocities are: $\sim 2.3 \times 10^{-3}$ cm/s, $\sim 10^{-2}$ cm/s, and $\sim 8 \times 10^{-2}$ cm/s respectively. Had particles with diameters larger than 100 μm been part of the discharge a Rubey or similar equation relating diameter (Dietrich, 1986) to settling velocity would then have had to have been used. An assumption that discharge particulates do not form agglomerates by flocculation after overflow is implicitly assumed. Agglomeration might accelerate settling. The comparison of observations with the model results assuming no agglomeration, however, prove to be adequate.

Horizontal diffusivities, K_x and K_y, are assumed to be equal, constant, and have a value of 2.0 m^2/s, consistent at the horizontal length scale of the plume with the data summarized by Okubo (1971). The vertical diffusivity, K_z, was given a value of 5 cm^2/s for particulates of 5 and 10 μm diameter and a value of 11 cm^2/s for particulates of 30 μm diameter.

Model advection velocities were based on current meter measurements during each experiment. Current speeds were taken to be time invariant during the simulation period of 1.5 hours. Speeds averaged over plume observation intervals at measured depths (e.g. Fig. 6) were interpolated to model levels using a parabolic equation

$$|u(z)| = |u_0|(1 - \delta(z/h))^2 \tag{2}$$

where $|u(z)|$ is the horizontal current speed at depth z, $|u_0|$ is the speed at the sea surface, z is the vertical coordinate, h is the total depth, and δ is a fitting coefficient. The dashed lines in Fig. 6 represent the fit of this parabolic form to the data of Cases A and B. The direction of currents for the model during each 1.5-hr simulation interval was also based on the current meter data, but current directions were adjusted at each computational time step (10 min) to match the current direction of the observations.

The model source term, Q, was given a vertical, fractional distribution, based on plume center line observations (Table 5). The source was taken to be a continuous point source in the horizontal plane. The absolute magnitude of the source along the track was based on the discharge data taken aboard the dredging ship.

The solution of Eq. 1 with the given boundary and source conditions was derived using a finite element formulation (e.g. Nakata, 1984) for the horizontal directions and multilayer scheme in the vertical direction. The finite element grid employed is shown in Fig. 7. The analytical area was determined by consideration of the operating areas of the dredger and the observing boats. The length of the element sides vary from 11.25 to 200 m. Near the source of turbidity the plume is so narrow that small elements are needed to resolve particulate distributions. The element size is coarser in regions where the plume has been broadened by time. The "L" shape of the smaller elements of the grid is needed to capture the details of the plume at an early age.

In the vertical direction, the nominal depth of the dredging area (15 m) was divided into 7 levels of unequal size. Level interfaces were designated at 2, 5, 6, 9, 12, and 14 m depths. The inequality of the level thicknesses better resolves the concentration at the depth of near-surface discharge (5.5 m). Overflowing water is introduced into the third level between 5 and 6 m, and the dredgehead is located in the seventh level.

TABLE 5. Computational conditions.

Items	Contents	Notes
Analytical area and finite elements	Shown in Fig. 7	
Velocity fields	e.g. Fig. 8	
Load of SS	Case A: 87.5 mt Case B: 131.5 mt	Reevaluated to 12.2 and 9.2 mt using Fig. 9.
Diameter of SS	5 μm, 10 μm, 30 μm	Multiple diameters are taken into account.
Vertical distribution of load	Shown in Table 4	
Diffusion coefficients	$K_x = K_y = 2.0 \times 10^4$ cm²/s $K_z = 5.0$ cm²/s $K_z = 11.0$ cm²/s for 30 μm diameter	According to trial computations
Duration of simulation	90 minutes	
Time increment	10 minutes	

Given the measured current directions, the depth-interpolated current speeds (Eq. 2), and the finite element grid of Fig. 7, the current field over the domain of calculation was constructed. An example of the velocity field at three depth levels for a single time step is shown in Fig. 8. The horizontal velocities were taken to be homogeneous and isotropic at each depth level and at each time step, but the velocity fields were allowed to change direction but not intensity over the period of each simulation. The length of simulation was 90 minutes and the time step was 10 min. A summary of the computational conditions are shown in Table 5.

4. INTERCOMPARISON OF MODEL AND OBSERVATIONAL RESULTS

Distributions of suspended solids for the experiments were calculated using the model and measured conditions (current speed and direction, source histories). Modeled suspended solids distributions were the sampled at points in the grid where the suspended solids samples had been taken by the survey boats. A comparison of the calculated and observed profiles, both vertical and horizontal, follow.

Before showing the results plotted against depth or distance, however, the results are first given in a correlation plot between measured and modeled concentrations (Fig. 9) for Cases A and B. The computed concentrations generally show much higher values than the observed ones.

The correlation between the results is quite strong, however, with correlation coefficients close to one (Fig. 9). The constant in each regression (approximately 3.3 mg/l) has a value within the range of the background suspended particulate concentration (1.3-9.2 mg/l). This relationship shows the computed and observed results to be in good agreement except for an overall normalization of model concentrations. In other words, Fig. 9 suggests that the magnitude of the initial loadings used in the model, but derived from the data taken aboard the dredger, are too high. Using the result of Fig. 9, it is estimated that the initial loadings are 12.2 mt and 9.2 mt for Cases A and B. These values are smaller than the estimates from the dredge ship (87.5 and 131.5 mt; Table 3) by an order of magnitude.

After discharge rates are revised downward in accordance with the result above, the computed and measured results are in good agreement. Fig. 10 compares vertical profiles of measured and modeled data at the plume center line, as determined by the drogues, for both Cases A and B. These profiles show the decrease in solids concentration with time. No readily recognizable differences in profiles between dredging without ATS (Case A) and dredging with ATS (Case B) occur. Concentrations return to background levels at the end of the 1.3-1.5-hr observation periods.

Profiles across the plume at depth also show good correspondence between observed and computed results (Fig. 11). Plume widths and peak concentrations match well. These transects show the decrease in maximum suspended solids concentrations from 50-60 mg/l to the background levels of about 3-5 mg/l over the period of the measurements. The profiles also show significant horizontal dispersion, which is responsible for much of the decrease in concentration. This is to be expected when the effluent is composed primarily of fine particles, 80% of which (<35 μm, Fig. 4) can be expected to settle no farther than 4.5 m over a 1.5-hr observation period. Thus, almost all changes in concentration must be the result of horizontal and vertical dispersion rather than settling.

Comparison of the results of the field test with and without ATS (Fig. 10 and 11) show no conclusive differences. These observations and data analyses *en toto* do not lend themselves to discerning the effectiveness of the ATS system in reducing the dispersion of overflow solids from hopper dredging.

5. EVALUATING THE EFFECTIVENESS OF ATS

In order to compare quantitatively the system results with and without ATS, a numerical test was conducted. Suspended solids concentrations were calculated with the model under identical discharge and oceanic conditions for the two cases. The difference between the two computations was only the vertical distribution of the discharge (Table 4): for dredging with ATS, solids were preferentially injected into the water column at depths below 5.5 m; for dredging without ATS, more of the solids were distributed between the surface and 6 m.

These additional computational conditions were imposed on both simulations: Diffusion coefficients and settling velocities distributions were identical, as was the amount of discharge (10 mt); the current velocity field for both cases was taken to be that of Case A; the discharge was a point source in the horizontal directions, rather than a line source horizontally as it was for the plume calculation associated with the field data analyses.

A comparison of results with and without ATS are given in Fig. 12. These are quantitatively similar, though examination in detail shows that the near-surface water column is slightly more concentrated in the case without ATS, as to be expected. More explicative of the differences are the numerical values at different levels in the water column (Table 6). These show the quantity of solids in mt in each model layer. Concentrations were integrated over the horizontal and vertical extent of the model for each layer to arrive at these results. These values can be compared to the total amount of solids (10 mt) introduced into the water column at the initial time of the calculation. Note that the initial vertical distribution for both cases is also given in Table 6.

One sees that the quantity settled to the bottom after 90 minutes without ATS is 9.5% of the initial mass whereas with ATS the quantity is 11.9%. This low percentage of redeposition in both cases is the result of the small sizes and hence settling velocities of particles that are dredged in this area. Over the same time interval concentrations in the surface layers decrease to 33% of their initial values in both cases. Concentrations near the bottom increase except for the bottom-most layer which loses solids suspended by the dredgehead to deposition. The total amount of suspended solids in the computational grid plus that lost to deposition also decreases in time. This indicates that advection and diffusion are moving particles beyond the calculational grid boundary. In the case without ATS 23% of the particulates have moved beyond the grid boundary after 90 minutes, whereas in the case with ATS only 19% have. This difference is the result of more solids being situated in the near-surface layers when ATS is not used and the fact that the largest currents are found there. These currents move the near-surface solids farther and more quickly than solids that remain at the discharge depth (5.5 m) and below.

The ratio of the concentrations at various levels over time are shown in Fig. 13. These show that at the initial time there are more particulates below and less particulates above 9 m with ATS than without it. This result reflects the choice of the initial distributions that were based on test measurements (Table 4). The ratio of concentrations in the upper layers stays nearly constant over time. Though solids are more concentrated in the upper water column for dredging without ATS, the percentage decrease of concentrations in the upper water column is about the same. In the lower water column, on the other hand, the actual concentrations tend toward equality. This is the result of particles settling and diffusing vertically into the lower water column from above. In the situation without ATS, the very lightly loaded layer centered at 10 m fills with solids from above and, to a lesser extent, from below.

TABLE 6. Simulated changes over time of layer and grid-integrated suspended solids concentration (mt) with and without ATS. Total initial mass over the entire water column is 10 mt. Results based on initial distributions that are points horizontally but are vertically distributed as in Table 4. Bottom accumulation load and total amount of sediment remaining in the analytical area are also given.

time course (min)	Suspended solid (mt) per meter							Total suspended solids (mt) in intervals:		accumulated on the bottom (mt)	amount of sediment within the area (mt)
	0.5 - 1.5 m	3.0 - 4.0 m	5.0 - 6.0 m	7.0 - 8.0 m	10.0 - 11.0 m	12.5 - 13.5 m	14.0 - 15.0 m	0.0 - 12.0 m	0.0 - 15.0 m		
Without ATS											
0	0.792	0.865	0.948	0.892	0.382	0.000	1.052	8.949	10.000	--	10.000
10	0.723	0.852	0.920	0.887	0.415	0.113	0.791	8.828	9.841	0.156	9.997
20	0.665	0.833	0.895	0.879	0.445	0.194	0.638	8.697	9.723	0.273	9.996
30	0.618	0.809	0.869	0.869	0.472	0.256	0.549	8.557	9.619	0.372	9.991
40	0.575	0.780	0.841	0.855	0.495	0.305	0.499	8.381	9.490	0.464	9.954
50	0.530	0.740	0.807	0.834	0.513	0.344	0.472	8.126	9.284	0.555	9.839
60	0.478	0.684	0.760	0.800	0.522	0.374	0.458	7.732	8.938	0.649	9.587
70	0.414	0.608	0.696	0.749	0.521	0.397	0.452	7.158	8.403	0.747	9.150
80	0.342	0.516	0.616	0.679	0.507	0.411	0.448	6.405	7.672	0.848	8.520
90	0.267	0.415	0.521	0.591	0.479	0.415	0.443	5.511	6.783	0.950	7.733
With ATS											
0	0.555	0.638	0.725	0.820	0.913	0.000	1.052	8.949	10.000	--	10.000
10	0.507	0.628	0.709	0.809	0.886	0.167	0.809	8.692	9.834	0.163	9.997
20	0.468	0.613	0.694	0.797	0.864	0.285	0.679	8.452	9.701	0.295	9.996
30	0.436	0.596	0.678	0.784	0.844	0.371	0.612	8.221	9.576	0.416	9.992
40	0.406	0.575	0.660	0.768	0.825	0.435	0.581	7.977	9.426	0.536	9.962
50	0.376	0.546	0.635	0.747	0.806	0.482	0.568	7.682	9.214	0.659	9.873
60	0.339	0.505	0.601	0.715	0.783	0.516	0.566	7.290	8.887	0.787	9.674
70	0.295	0.450	0.553	0.670	0.753	0.539	0.565	6.761	8.404	0.919	9.323
80	0.244	0.383	0.492	0.609	0.713	0.550	0.564	6.092	7.757	1.053	8.810
90	0.191	0.309	0.419	0.532	0.661	0.551	0.561	5.307	6.969	1.187	8.156

Table 7 shows the differences between the two systems in terms of the sedimentation areas and resedimentation loads. Over the 90 minute simulation the amount of resedimentation is about 10%. Resedimentation exceeding 20 g/m^3 occurs over a region of about 3000 m^3 in both cases. For lesser amounts of sedimentation cover, the system with ATS covers more area within the calculational domain. This is to be expected since the initial condition with ATS places more solids nearer the seabed. In both cases the small size of the particles allows suspended solids to drift out of the calculational area. These estimates are made with a model having no boundary layer. Inclusion of a boundary layer in the model would somewhat reduce the lateral excursion of solids before redeposition.

TABLE 7. A comparison of the sedimentation areas and resedimentation loads with and without ATS. Sedimentation mass per unit area is designated by μ.

levels of accumulated sediment per unit area (g/m^2)	sedimentation area (m^2)			
	with ATS	without ATS	difference: with ATS vs. without ATS	ratio: with ATS / without ATS
$0.0 < \mu \leq 2.5$	3,733,550	3,795,721	– 62,171	0.9836
$2.5 < \mu \leq 5.0$	74,219	38,594	35,625	1.9231
$5.0 < \mu \leq 10.0$	18,750	12,969	5,781	1.4458
$10.0 < \mu \leq 15.0$	5,468	5,000	469	1.0938
$15.0 < \mu \leq 20.0$	2,187	1,953	234	1.1200
$20.0 < \mu$	3,125	3,047	78	1.0256
TOTAL	3,837,300	3,857,284	– 19,983	0.9689

6. CONCLUSIONS

From the observed data, ATS qualitatively appears to be effective in reducing the turbidity of the surface layer. Numerical calculations are capable of reproducing the observed distributions to within an overall normalization constant. The discrepancy between absolute values of the model and measured concentration when shipboard discharge rates are used is likely the result of the rapidly varying discharge concentrations as evidenced in the measurements aboard the ship.

The model allows comparison of results under identical conditions of current and turbulence that cannot be attained in sequential experiments in the ocean. Those computations permit the differences of the use and non use of ATS to be assessed. They show increased deposition on the bottom of more than 25% using the ATS system. Additionally, the area of surface turbid water and the range of dispersion marginally decrease when ATS is used.

It is clear from these experiments that further reduction in the sediment dispersion will occur when the particulates, scrubbed of entrained air by an ATS system, are released much nearer the seafloor.

The numerical experiments are performed under a variety of assumptions, the most ambiguous of which may be estimating the vertical profile of suspended solids immediately following the passage of the dredge ship. To better evaluate the effectiveness of ATS, further field experiments and numerical experimentation are required.

7. ACKNOWLEDGMENTS

We thank the Marine Mining Panel of the United States–Japan Cooperative Program in Natural Resources for recognizing the need for an experiment of this type as well as for providing the coordinating mechanism that enabled this multi-agency experiment to take place. We also appreciate financial assistance from the U.S. Department of the Interior's Minerals Management Service.

8. REFERENCES

Batchelor, G.K. (1967): *An Introduction to Fluid Mechanics.* Cambridge University Press, London.

Dietrich, W.E. (1982): Settling velocity of natural particles. *Water Resour. Res., 18*(6), 1615-1626.

Marine Mining Panel (1984): Data report from an experiment to measure the dispersion of a hopper dredge discharge plume at Kanmon Channel, Japan. The United States-Japan Cooperative Program in Natural Resources, NOAA/Office of Ocean and Coastal Resource Management, Rockville, MD, unpublished data report.

Nakata, K. (1984): The three-dimensional diffusion model of suspended solids in sea water by using the finite element method. Unpublished report.

Ofuji, I., S. Waseda, and N. Ishimatsu (1977): Anti-turbidity overflow system for a hopper dredger, *IHI Engineering Review, 10*, 61-68.

Okayama, Y., and Y. Saotome (1980): Turbidity of sea surface by hopper dredges and effective preventions. Report to the 8th Joint Meeting, Marine Mining Panel, The United States-Japan Cooperative Program in Natural Resources, NOAA/Office of Ocean and Coastal Resource Management, Rockville, MD, unpublished report.

Okubo, A. (1974): Some speculations on oceanic diffusion diagrams. *Rapp. P-v. Réun. Cons. Int. Explor. Mer., 167*, 77-85.

FIGURES

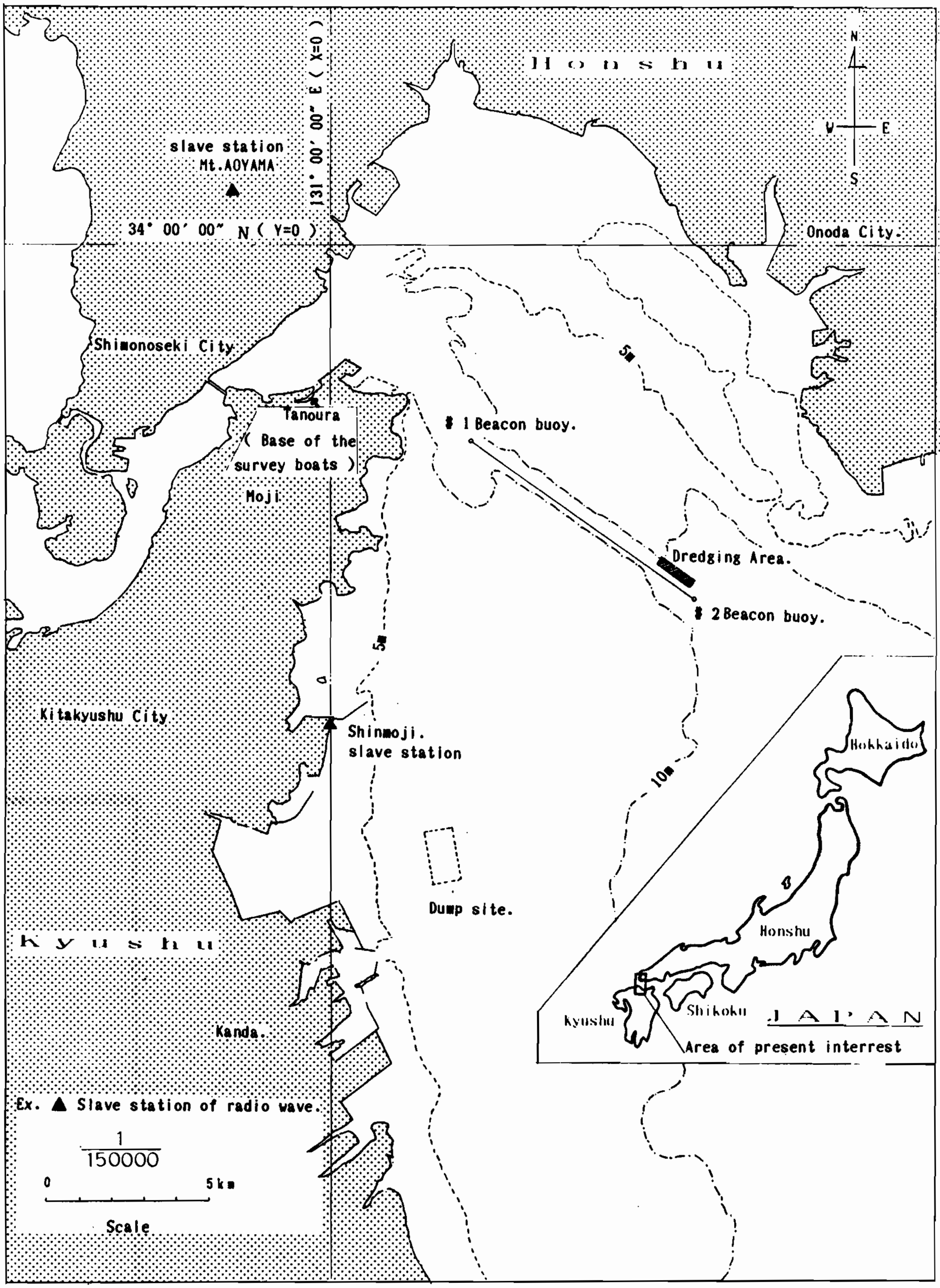

Figure 1. Location map of dredging area.

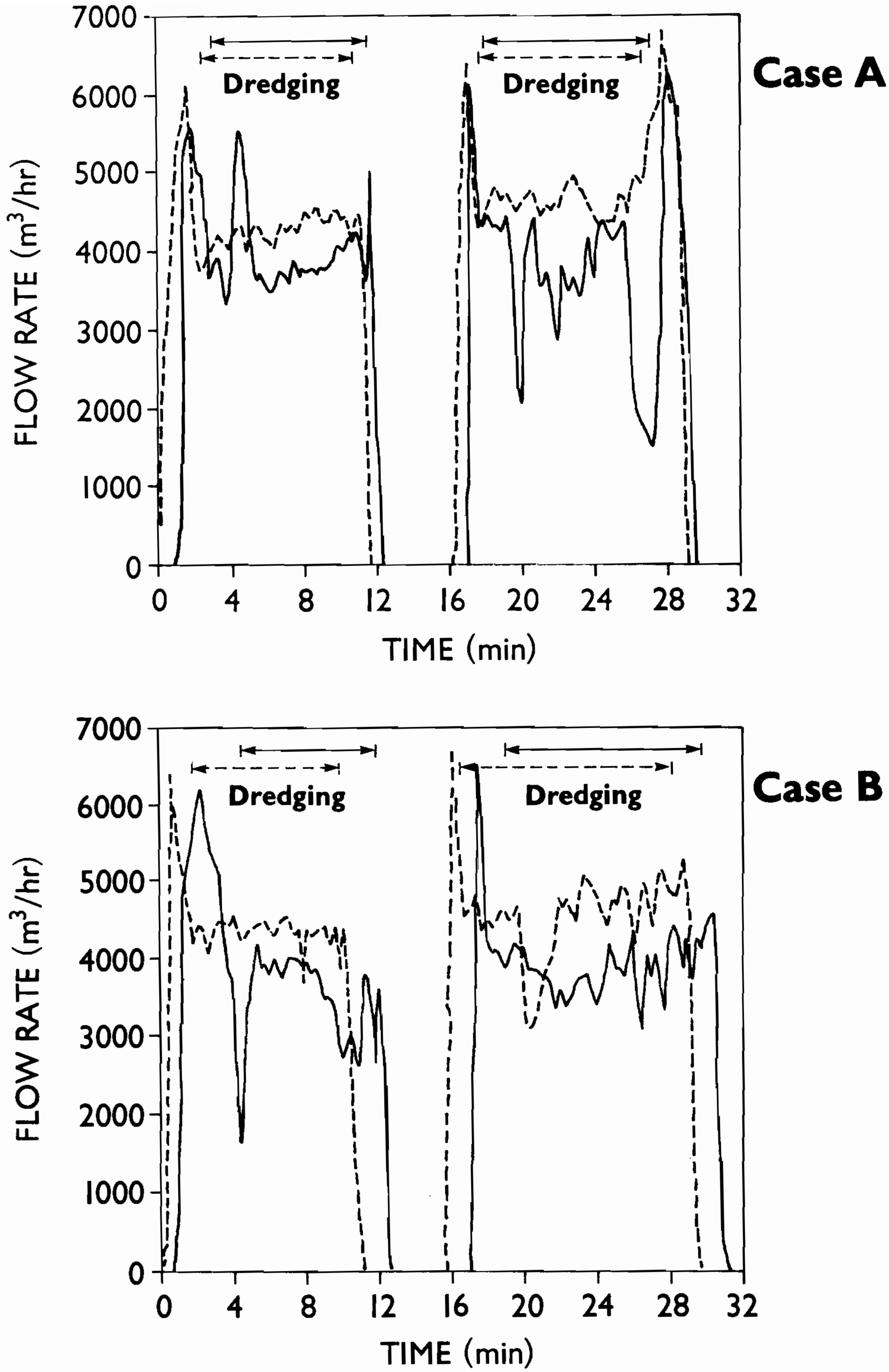

Figure 2. Flow rates through port (solid line) and starboard (dashed lines) side pumps of the hopper dredge KAIHO MARU during Experiment 4 (Case A) and Experiment 6 (Case B).

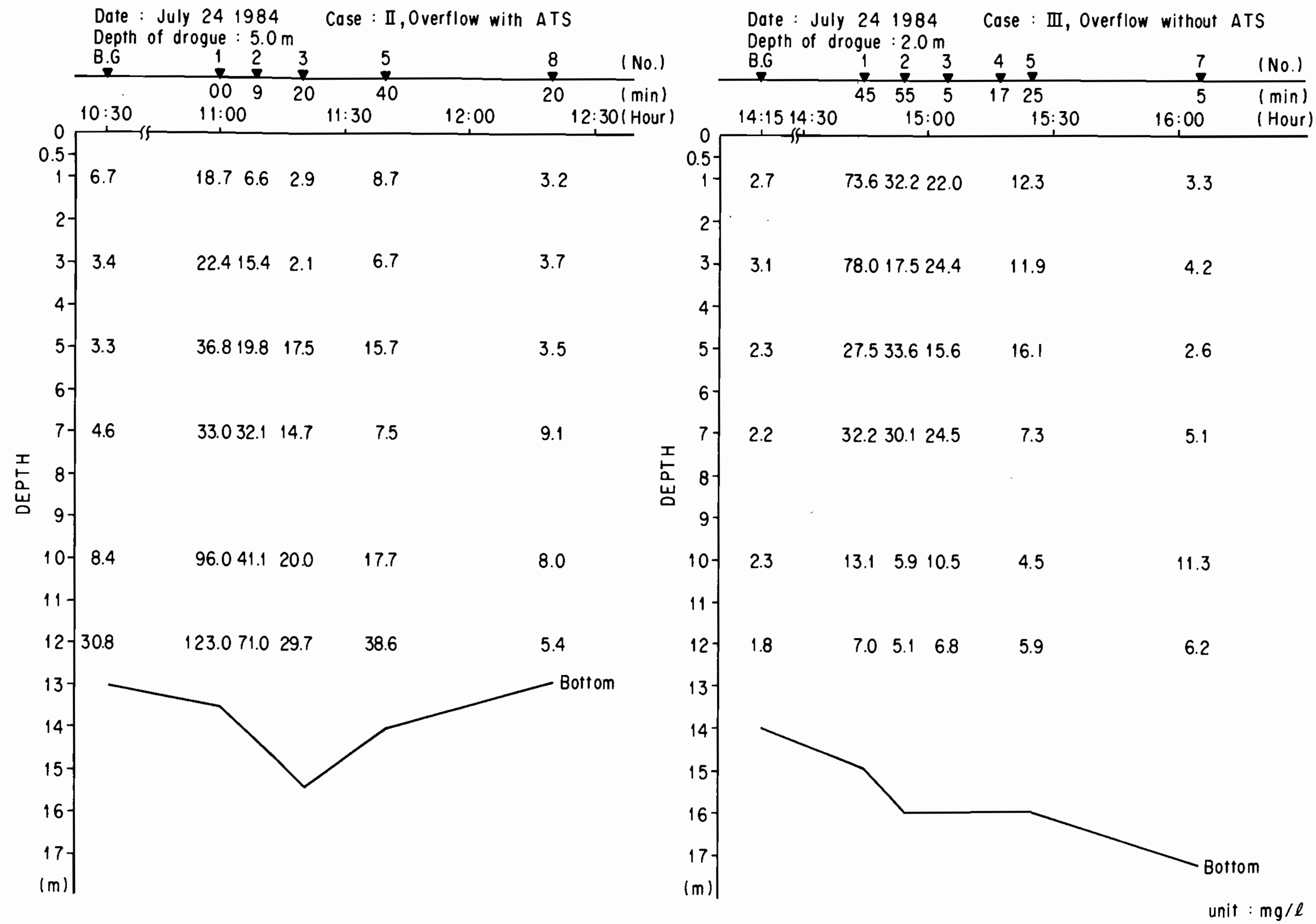

Figure 3a. Vertical distributions of suspended solids along the plume centerline for Experiments 3 and 4. Concentrations are in mg/l and the time of measurements is indicated.

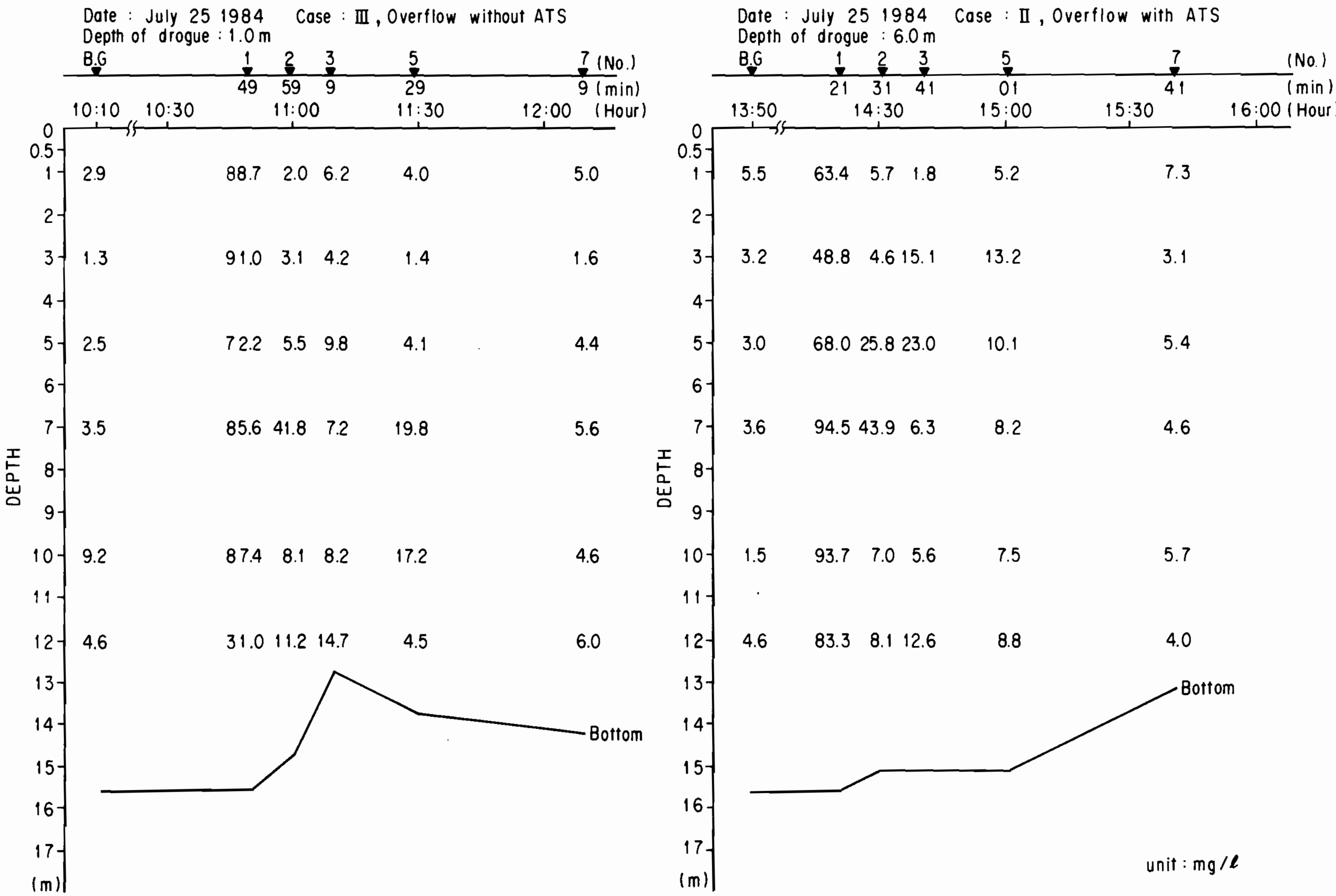

Figure 3b. Vertical distributions of suspended solids along the plume centerline for Experiments 5 and 6. Concentrations are in mg/l and the time of measurements is indicated.

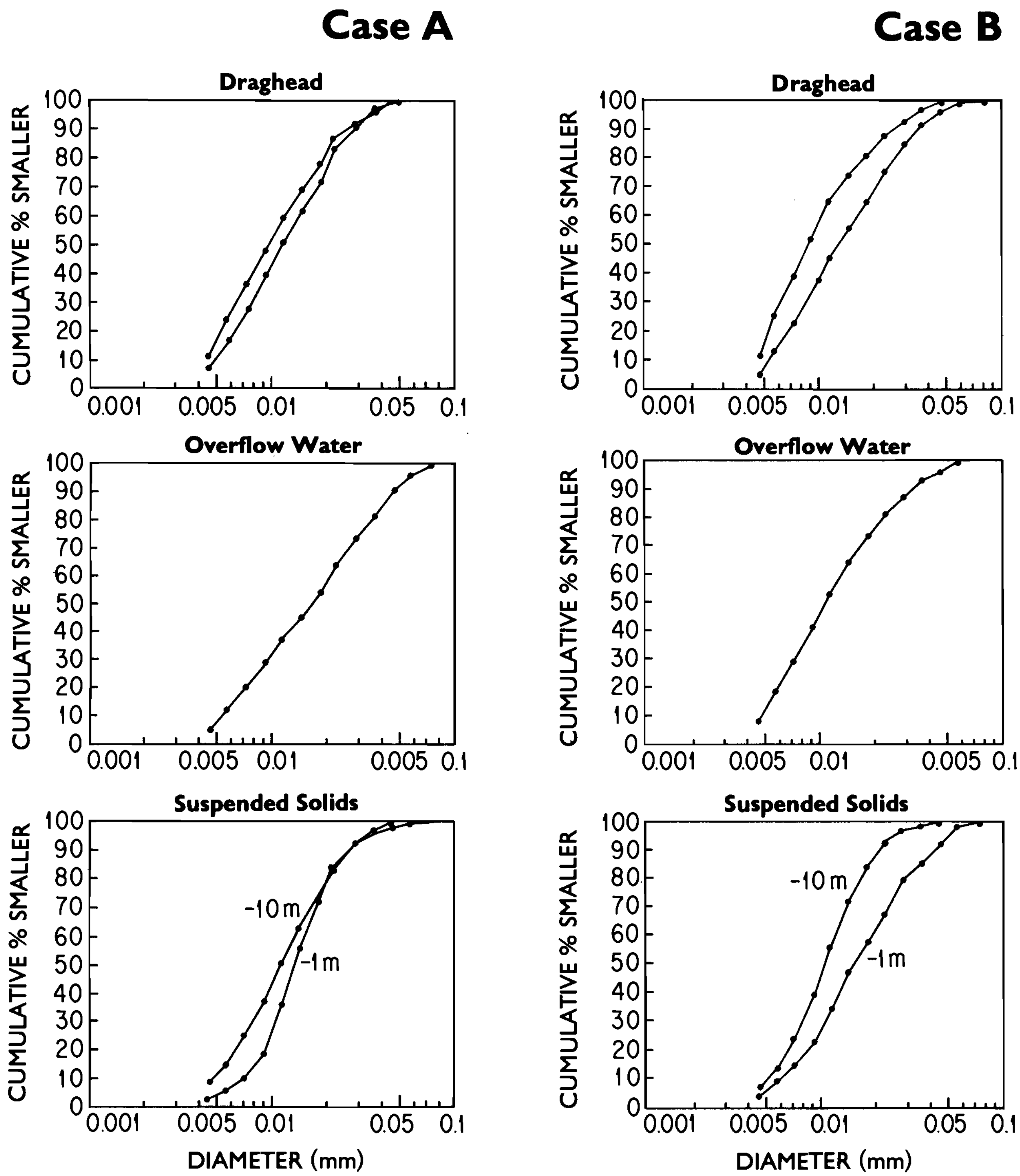

Figure 4. Cumulative size distributions for solids sampled at the dredgehead, in the overflow water, and in the plume for Cases A and B.

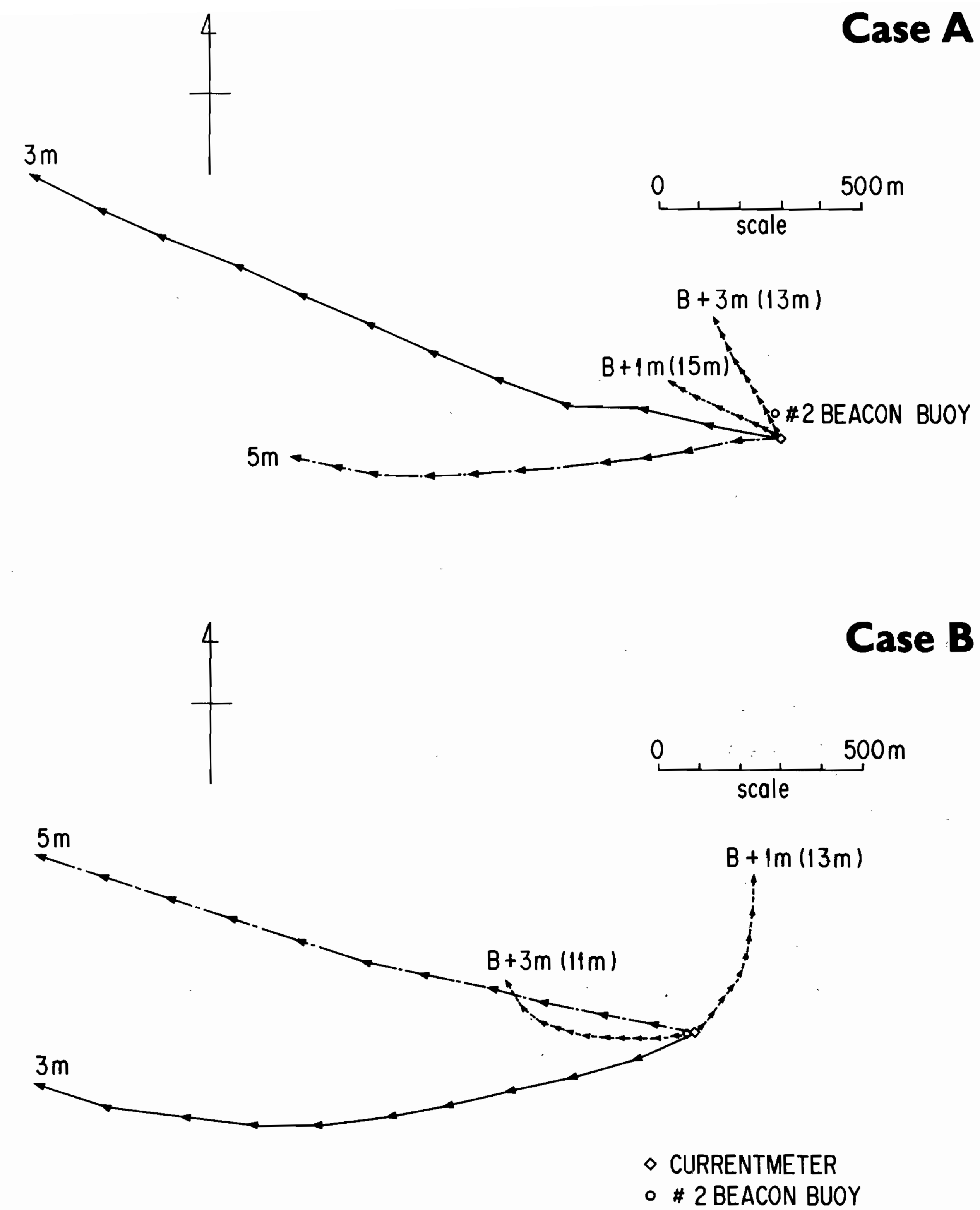

Figure 5. Progressive vector diagrams of currents in the dredging area for Cases A and B. Arrows denote 10-minute intervals.

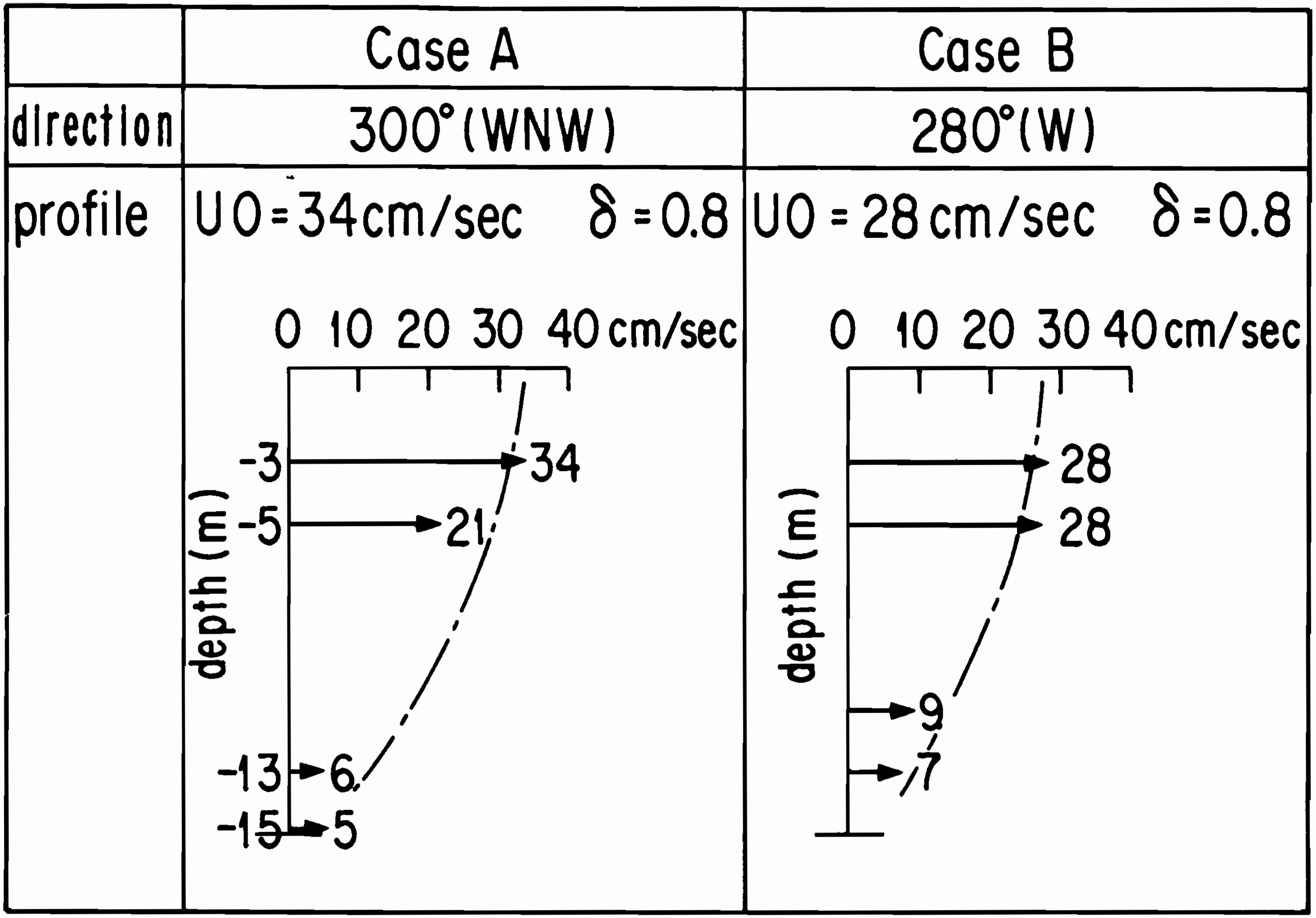

Figure 6. Average current speed and direction over the observational periods of Cases A and B. Broken line corresponds to fit of the speed data using Eq. 2.

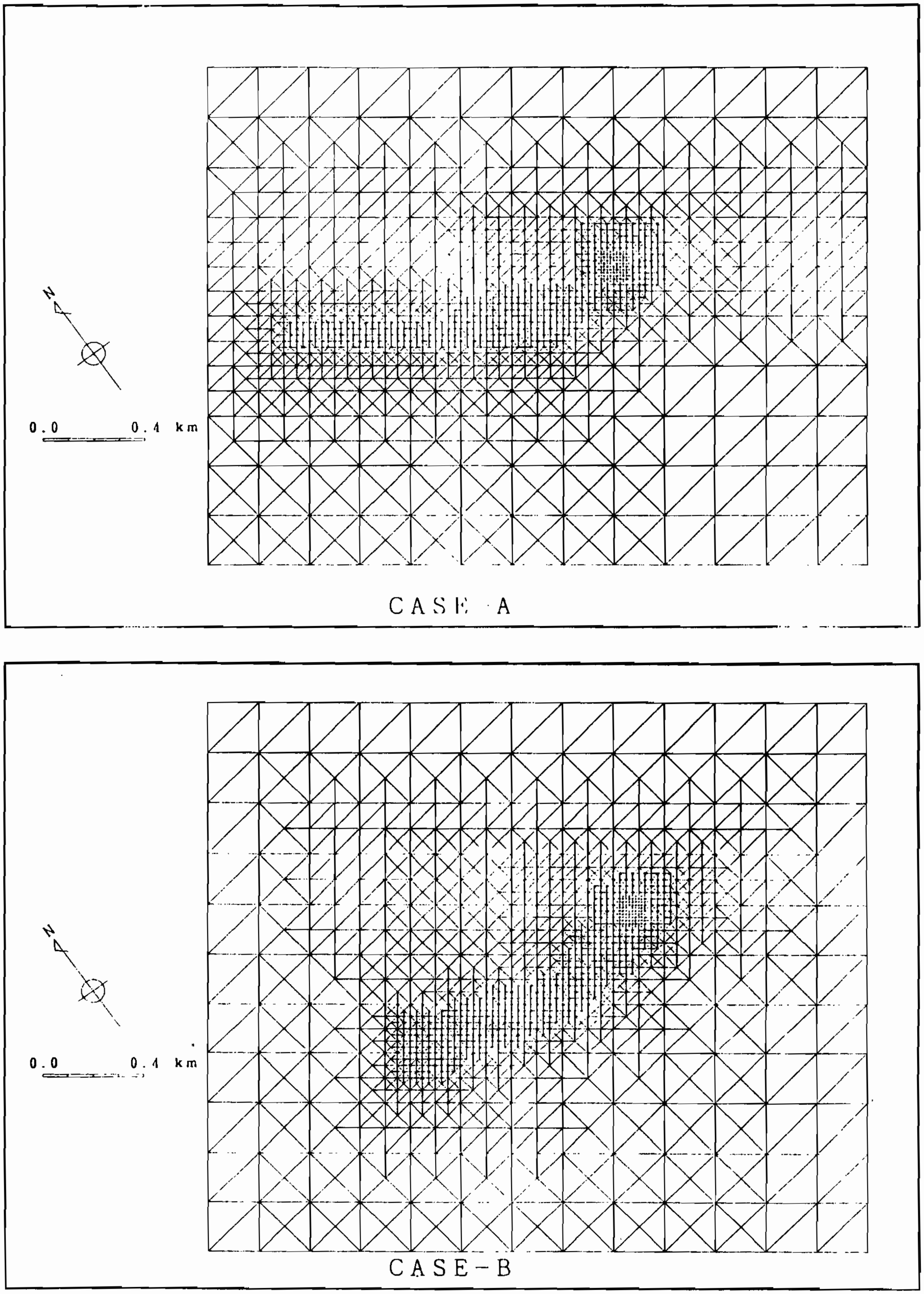

Figure 7. Finite element grids through the model dredge area for Cases A and B.

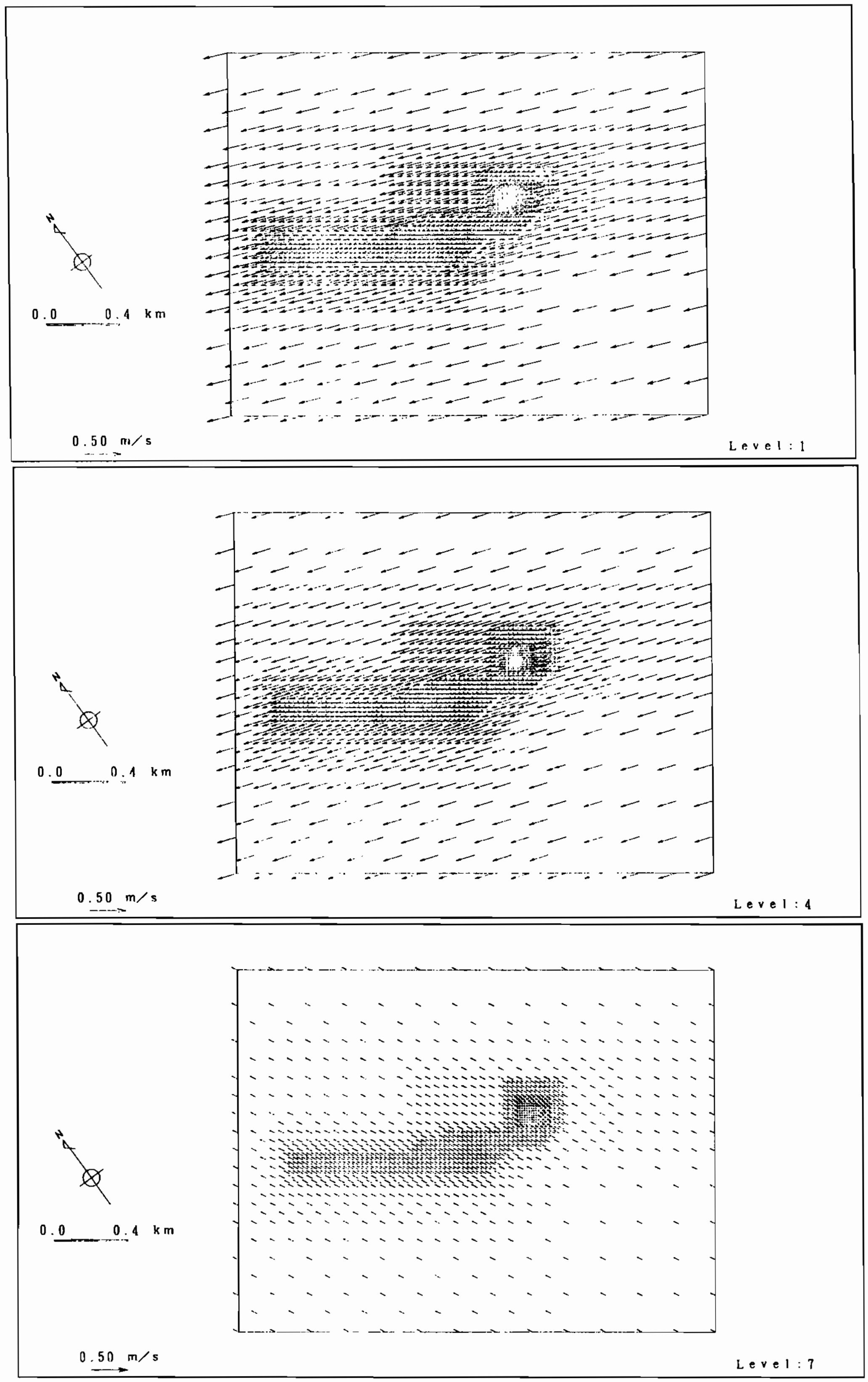

Figure 8. Examples of model velocity fields, here given at three depths and at 60 minutes after the simulation start time for Case A. Speed at each level is constant in time for each simulation, but current direction is allowed to vary in accordance with the field measurements.

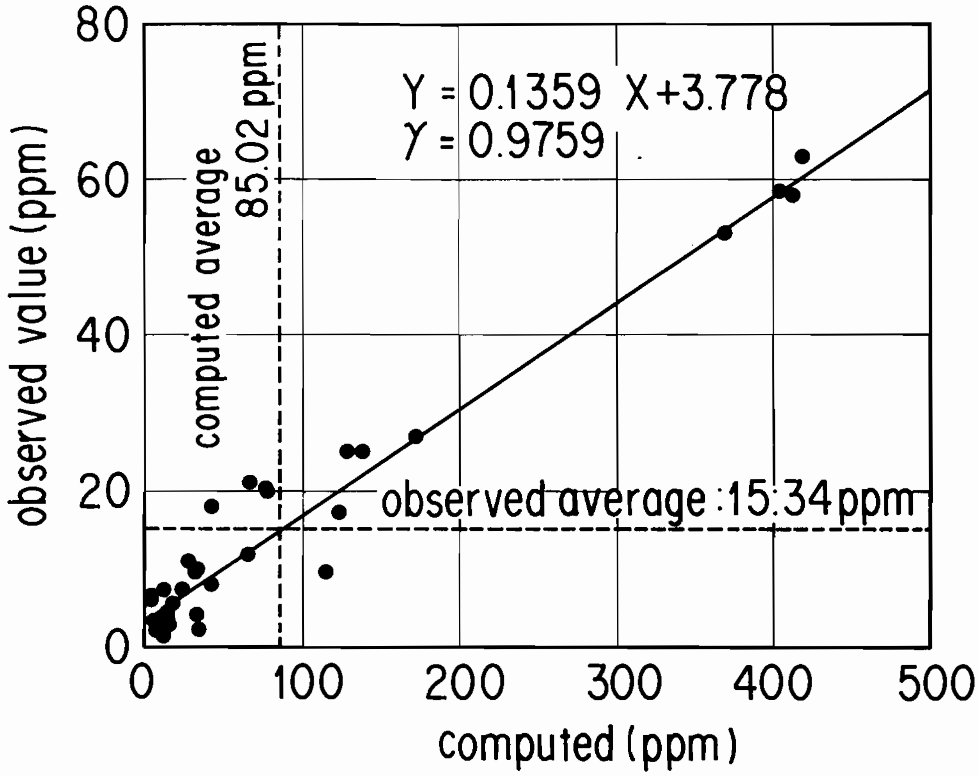

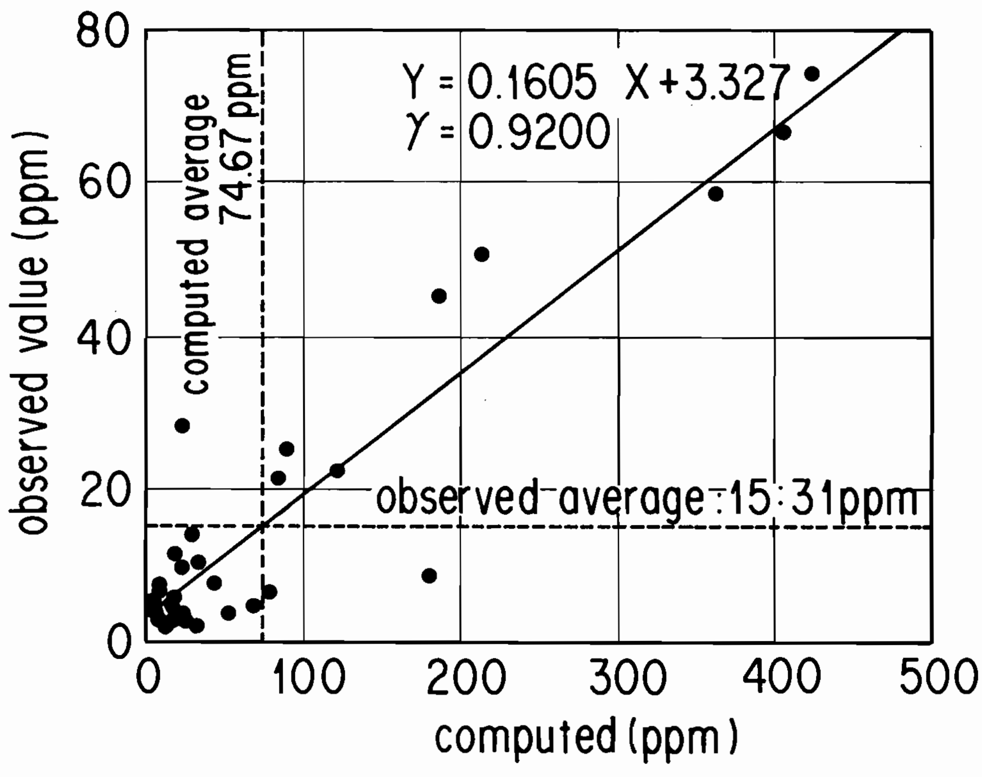

Figure 9. Comparison of concentration values from the model and measurements for Cases A and B. Model normalization was determined by the measured suspended solids discharge rates on the dredge ships.

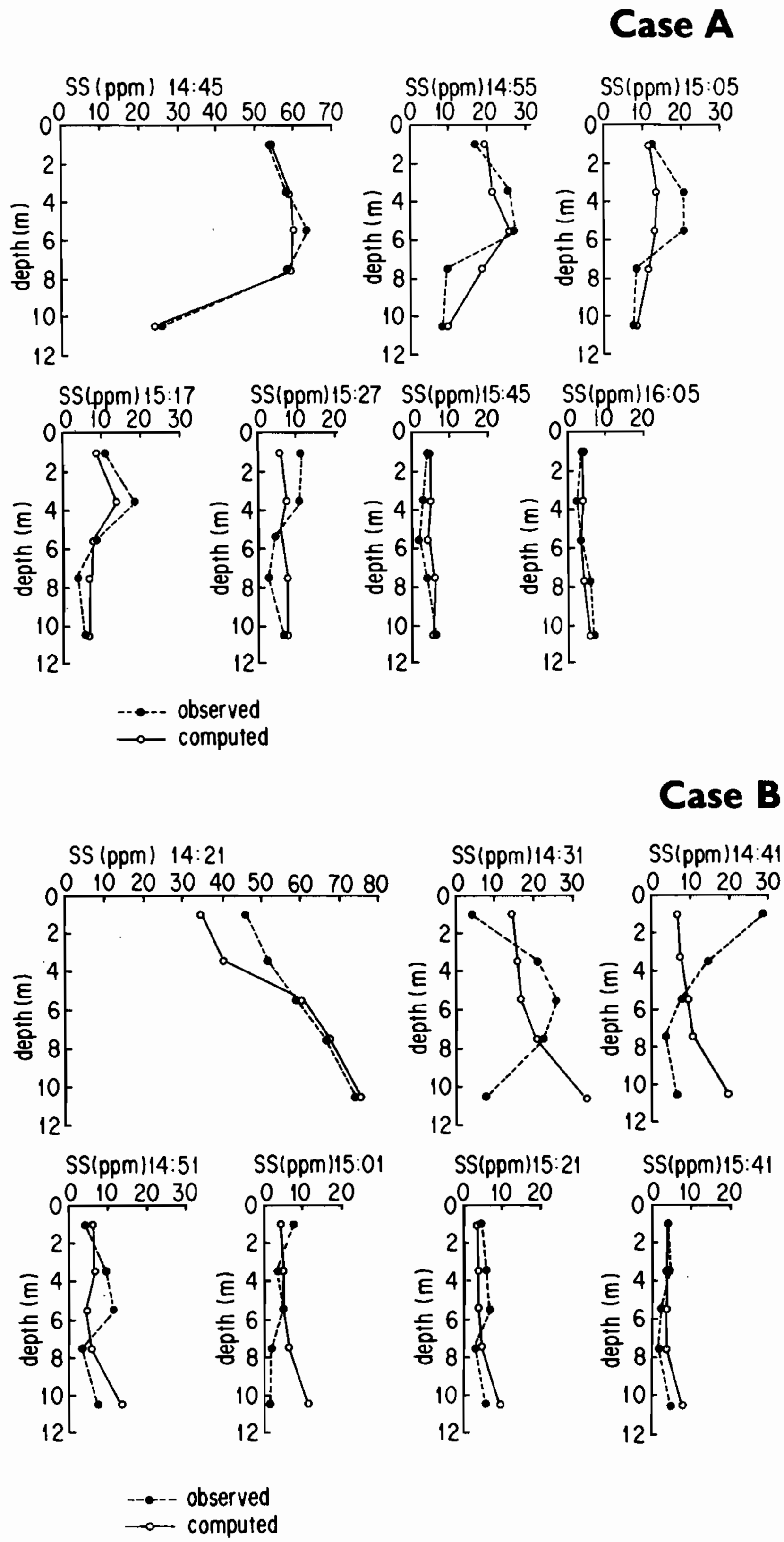

Figure 10. Vertical profiles of measured and model data for Cases A and B using revised discharge rates.

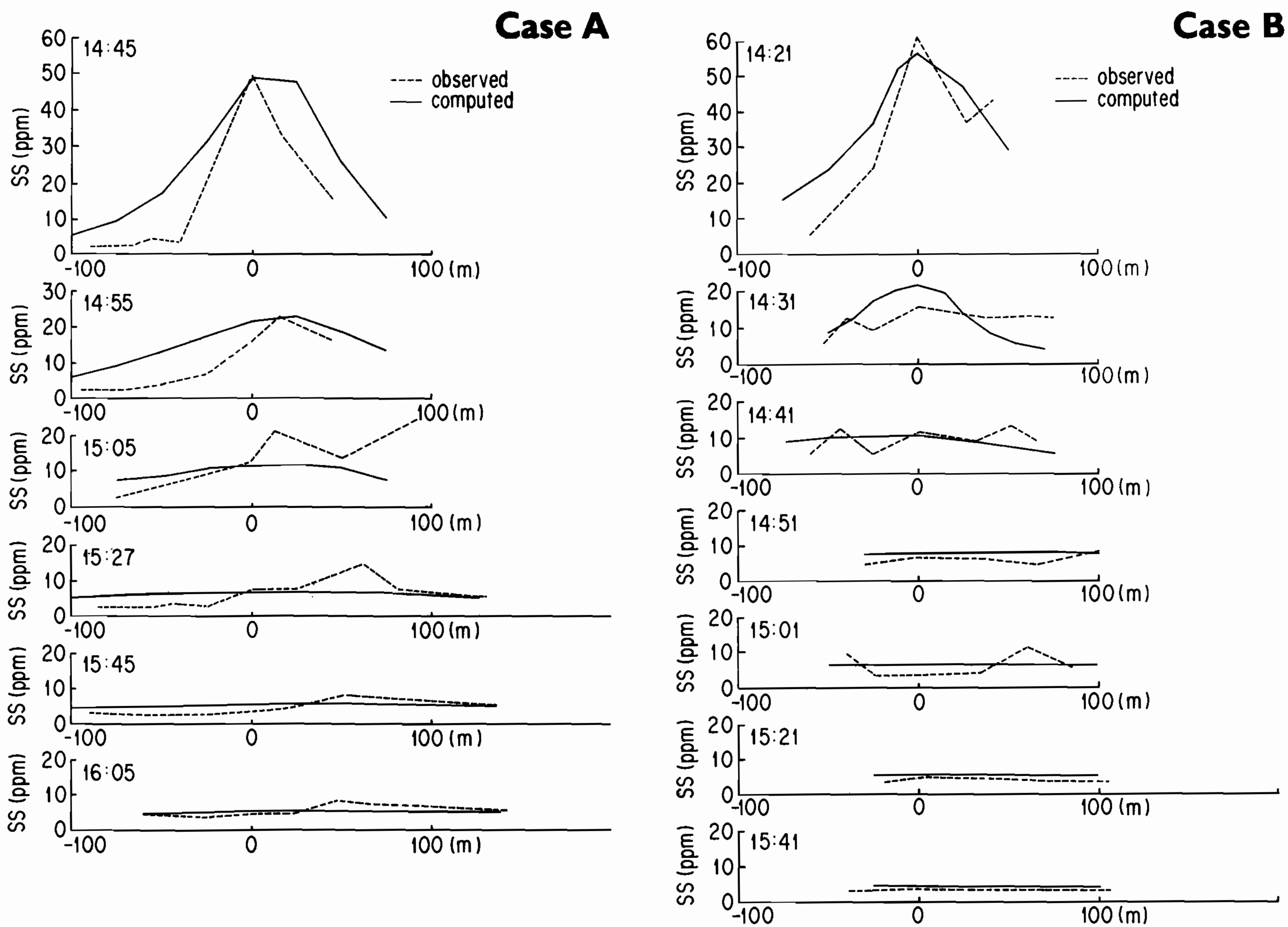

Figure 11. Horizontal profiles of measured and model data for Cases A and B using revised discharge rates.

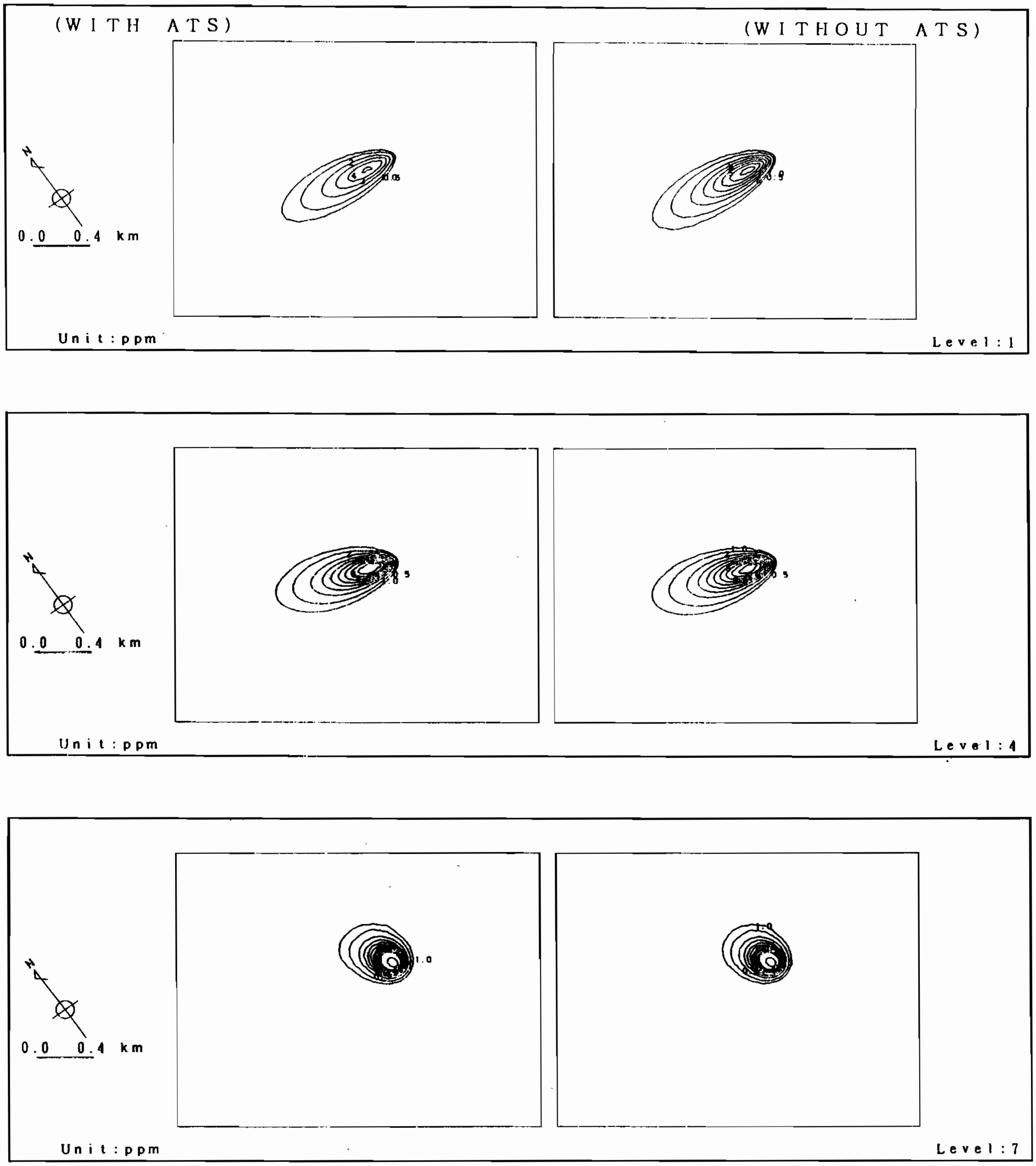

Figure 12a. Plume dispersion patterns at three levels with and without ATS after an idealized release of suspended solids 30 min after initiation of discharge.

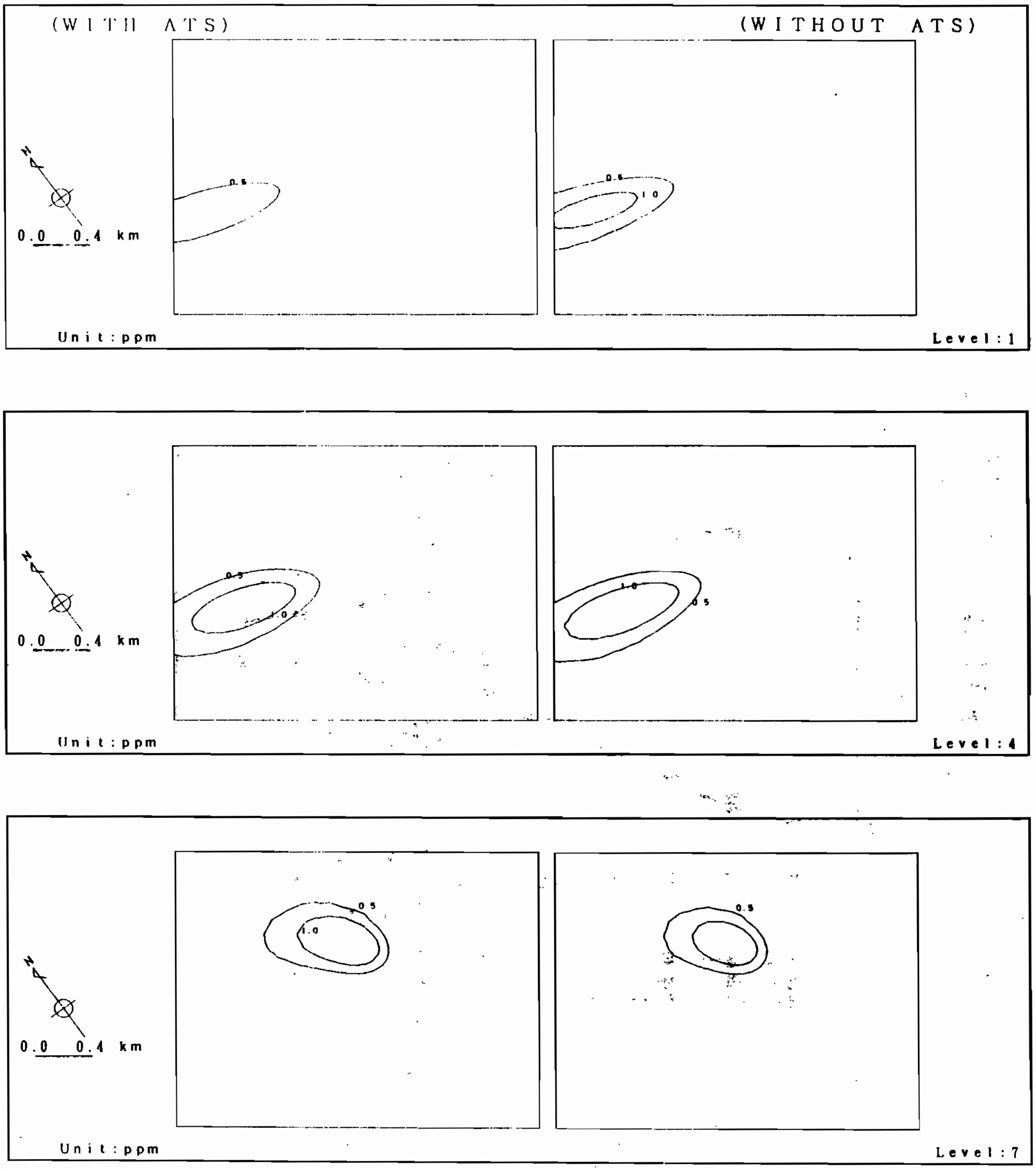

Figure 12b. Plume dispersion patterns at three levels with and without ATS after an idealized release of suspended solids 90 min after initiation of discharge.

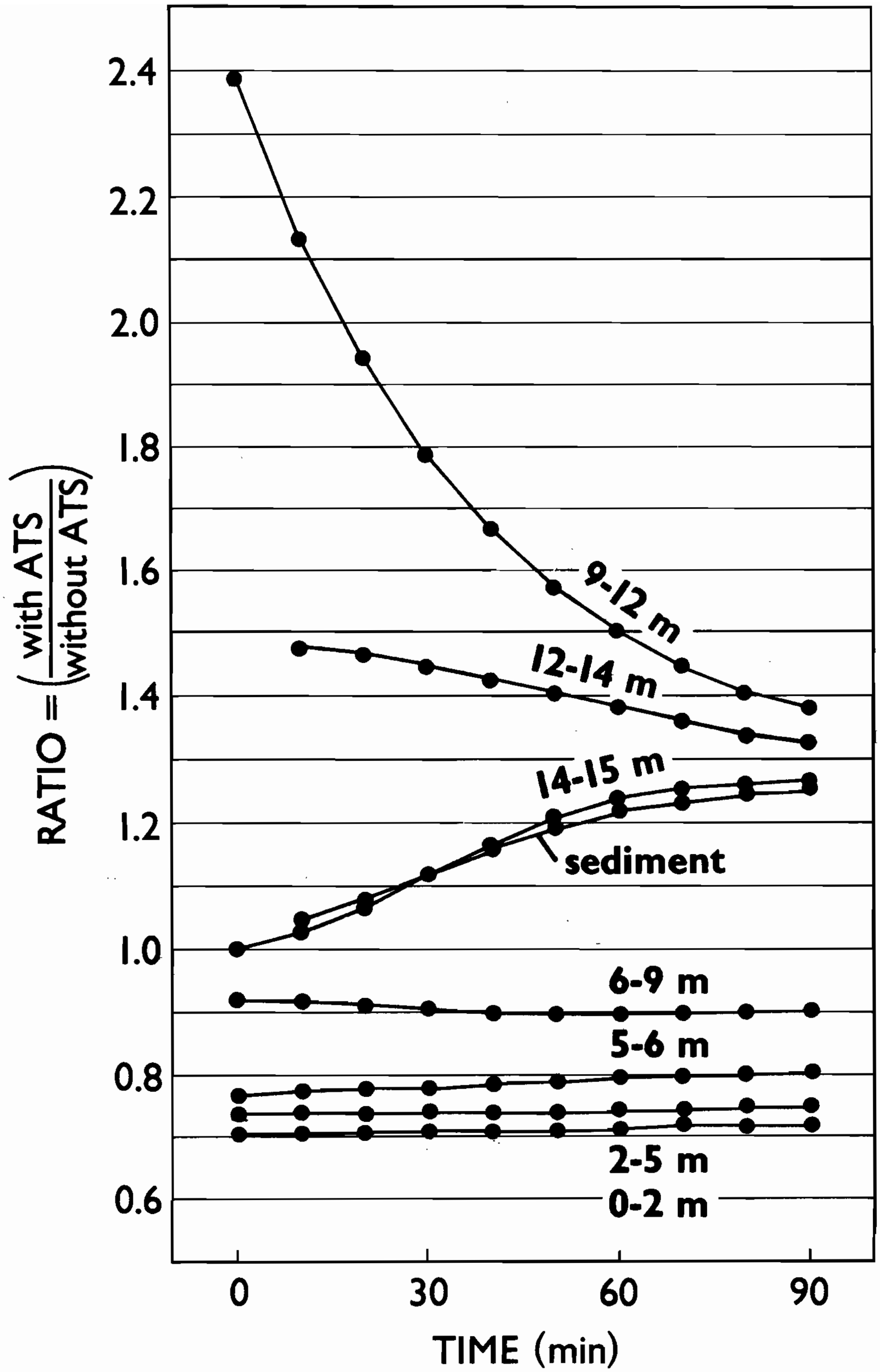

Figure 13. Ratios of suspended solids with and without ATS at each level for an idealized release of suspended solids.

☆ U.S. GOVERNMENT PRINTING OFFICE: 1989 — 673-002/92022